

arXiv:nucl-th/9812079v1 31 Dec 1998

# Quark Delocalization, Color Screening Model and Nucleon-Baryon Scattering

Guang-han Wu

*Radiation Center, Institute of Nuclear Science and Technology, Sichuan University, Chengdu, 610064, P. R.China*

LA-UR-98-5841

Jia-Lun Ping

*Department of Physics, Nanjing Normal University, Nanjing, 210097, P. R.China*

Li-jian Teng

*Radiation Center, Institute of Nuclear Science and Technology, Sichuan University, Chengdu, 610064, P. R.China*

Fan Wang

*Center for Theoretical Physics and Department of Physics, Nanjing University, Nanjing, 210008, P. R. China.*

T. Goldman

*Theoretical Division, T-5, Los Alamos National Laboratory, Los Alamos, NM87545, U.S.A  
(September 17, 2018)*

## Abstract

We apply the quark delocalization and color screening model to nucleon-baryon scattering. A semi-quantitative fit to N-N, N- $\Lambda$  and N- $\Sigma$  phase shifts and scattering cross sections is obtained without invoking meson exchange. Quarks delocalize reasonably in all of the different flavor channels to induce effective nucleon-baryon interactions with both a repulsive core and with an intermediate range attraction in the cases expected.

25.80.-e

25.10.+s

13.75.-n

25.40.-h

Typeset using REVTEX



## I. INTRODUCTION

QCD has acquired significant experimental support as the correct fundamental theory of the strong interaction. However in the low energy region, its nonperturbative nature makes it hard to use directly for the study of complicated systems such as hadron interactions and exotic quark states. QCD inspired models are generally used in these cases. Meson exchange models <sup>[1,2]</sup>, on the other hand, are quite successful in explaining the hadron interactions. But since the quark and gluon degree of freedom are completely integrated out and many phenomenological coupling constants and short-range phenomenology are involved in this model, it is hard to use it to make predictions of the properties of exotic quark states. Hybrid meson-gluon exchange quark cluster models have been developed by few groups <sup>[3–5]</sup> and have achieved a quantitative fit to the scattering data that accounts well for nucleon-baryon interactions <sup>[3]</sup>. However, in ref. [3] baryons are assumed to be so stiff that no internal distortion would be induced, no matter how close the interacting baryons are. The Hamiltonian used is a direct extension of that used in single hadrons. It is possible that some physics has been precluded by these assumptions a priori. For example, the QCD vacuum in between baryons can be expected to vary as the quark matter density increases as two colliding baryons approach each other and quark percolation between hadrons may occur at short distances. On the other hand, the color confinement interaction is screened at large distances due to excitation of quark-antiquark ( $q\bar{q}$ ) pairs, as has been shown by unquenched lattice QCD calculation <sup>[6]</sup>. Also, various kinds of multigluon exchange interactions cannot be included in two body confinement or the Fermi-Breit form for the interaction; nor can they be studied in the pure valence quark model of single hadrons. An example of such a three gluon exchange interaction, which is impossible for a  $q\bar{q}$  meson and does not contribute within a colorless  $q^3$  baryon but does contribute to hadron-hadron interactions and to multiquark states, has been discussed in ref. [7].

Recently, the proposed  $d'$  ( $IJ^P = 00^-$ ) dibaryon has been studied by Faessler's group <sup>[8]</sup>, who concluded that both bag and hybrid meson-gluon exchange models cannot obtain such a state with a mass as low as 2.06GeV. If the  $d'$  is proven to exist, that will argue strongly against the completeness of these models. Moreover, some well established facts are either impossible or hard to address within either the meson exchange or the hybrid meson-gluon exchange model approaches. For example, nuclear and molecular forces have been known to be similar for more than half a century <sup>[9]</sup>. If the nuclear intermediate range attraction is due to meson exchange, then the similarity would be accidental because the molecular force certainly cannot be due to electron-positron pair exchange. The nucleus as a collection of nucleons which has been proven to be a good approximation through the nuclear structure studies, which leaves a question as to why nucleus is not simply a collection of quarks.

A different approach has been developed by our group, which we call the quark delocalization, color screening model (QDCSM) <sup>[10]</sup>. It is aimed at including more of the physics needed for the study of exotic quark states. With the lessons <sup>[11]</sup> learned in earlier studies of such states in mind, we first tested our model on N-N scattering data <sup>[10]</sup>. We found that the QDCSM is able to produce both the N-N short range repulsion and intermediate range attraction simultaneously without invoking meson exchange. The similarity between nuclear and molecular forces thus obtains a natural explanation, i.e.,

the intermediate range attraction is due to distortion of the internal structure of the constituent nucleons (and atoms, respectively). Nuclear collections of  $6q$ ,  $9q$  and  $12q$  systems can be shown to be energetically favored when they have structures organized into something close to the conventional form of  $d$ ,  $^3H$ ,  $^3He$  and  $^4He$ . On the other hand, a  $6q$  system with  $IJ^P = 03^+$  quantum numbers is energetically favored to be in a six quark state,  $d^*$ , instead of two  $\Delta$ s. This state is predicted to be a narrow resonance with width of order MeV [12].

Only very limited experimental data is available for nucleon-hyperon (N-Y) scattering. Nevertheless it provides a further check of hadron interaction models. Here we report the results of applying the QDCSM to N-Y scattering. We should emphasize immediately that we are not so ambitious as to expect to achieve a quantitative fit to all nucleon-hyperon scattering with an almost parameter free model; more modestly, we only seek to test further whether the QDCSM contains basically the right physics.

## II. QUARK DELOCALIZATION AND COLOR SCREENING MODEL

We present a two baryon system as an example to illustrate the QDCSM. The generator coordinate method (GCM) is used to describe the  $6q$  system. The GCM basis wave function (WF) is assumed to be

$$\Psi(1 \cdots 6) = \mathcal{A}[\psi_{B_1}(123)\psi_{B_2}(456)]_{ST}, \quad (1)$$

$$\psi_{B_1}(123) = \chi_{c_1}(123)\eta_{S_1 T_1}(123)\psi_L(1)\psi_L(2)\psi_L(3), \quad (2)$$

$$\psi_{B_2}(456) = \chi_{c_1}(456)\eta_{S_2 T_2}(456)\psi_R(4)\psi_R(5)\psi_R(6), \quad (3)$$

where  $\mathcal{A}$  is the normalized antisymmetrization operator and  $\chi_{c_i}, \eta_{S_i T_i}$  ( $i = 1, 2$ ) are color, spin-isospin WFs.  $[ ]_{ST}$  means that  $S_1 T_1, S_2 T_2$  are coupled to channel spin  $S$  and isospin  $T$ .  $\chi_{c_i}$  is always the  $3q$  color singlet state.  $\eta_{S_i T_i}$  is the  $SU_6^{\sigma\tau}$  symmetric spin-isospin WF for the N-N channel, but for  $\Lambda$  and  $\Sigma$ , we use the  $uds$  spin-flavor asymmetric hyperon WF,

$$\begin{aligned} \Lambda \uparrow (456) &= \sqrt{\frac{1}{2}}(u_4 d_5 - d_4 u_5)s_6 \sqrt{\frac{1}{2}}(\uparrow_4 \downarrow_5 - \downarrow_4 \uparrow_5) \uparrow_6 \\ \Sigma^0 \uparrow (456) &= \sqrt{\frac{1}{2}}(u_4 d_5 + d_4 u_5)s_6 \sqrt{\frac{1}{6}}(2 \uparrow_4 \uparrow_5 \downarrow_6 - \uparrow_4 \downarrow_5 \uparrow_6 - \downarrow_4 \uparrow_5 \uparrow_6), \end{aligned} \quad (4)$$

where the arrows refer to the quark and overall baryon spin, and antisymmetrization will be applied to the five  $u, d$  quarks only for N- $\Lambda$  and N- $\Sigma$  channels. This choice explicitly distinguishes  $s$  quarks and allows for flavor symmetry breaking effects to be calculated more easily, but the results are the same as those which use an  $SU_6^{\sigma f}$  symmetric baryon WF and totally antisymmetric six quark states.

Our spatial WFs take the form

$$\psi_L(\vec{r}) = (\phi_L(\vec{r}) + \epsilon \phi_R(\vec{r})) / \sqrt{1 + \epsilon^2 + 2\epsilon \langle \phi_L | \phi_R \rangle}, \quad (5)$$

$$\psi_R(\vec{r}) = (\phi_R(\vec{r}) + \epsilon \phi_L(\vec{r})) / \sqrt{1 + \epsilon^2 + 2\epsilon \langle \phi_L | \phi_R \rangle}, \quad (6)$$

$$\phi_L(\vec{r}) = \left(\frac{1}{\pi b^2}\right)^{3/4} e^{-\frac{(\vec{r}-\vec{s}_1)^2}{2b^2}}, \quad (7)$$

$$\phi_R(\vec{r}) = \left(\frac{1}{\pi b^2}\right)^{3/4} e^{-\frac{(\vec{r}-\vec{s}_2)^2}{2b^2}}, \quad (8)$$

where  $b$  is the size parameter of baryon.  $\vec{s} = \vec{s}_2 - \vec{s}_1$ , which is the separation of two reference centers, plays the role of the generator coordinate in our model. The only difference from the usual GCM basis WF is found in the single quark orbital WF eq.(5, 6): A delocalization parameter  $\epsilon(s)$ , which will be determined variationally by the six quark dynamics for each separation  $s = |\vec{s}|$ , has been introduced to describe the mutual percolation of quarks originally confined in different baryons. This basis WF includes the six quark bag-model-like WF ( $\epsilon = 1$  case, which is spherical only for  $\vec{s} = \vec{0}$ ) and the usual quark cluster model WF ( $\epsilon = 0$  case) as two extremes. Note that intermediate configurations corresponding to mutually distorted baryons are allowed within the variational Hilbert space.

The Hamiltonian of the six quark system is taken as

$$H(1 \cdots 6) = \sum_{i=1}^6 (m_i + \frac{p_i^2}{2m_i}) + \sum_{i < j=1}^6 (V_{ij}^c + V_{ij}^G), \quad (9)$$

$$V_{ij}^G = \alpha_s \frac{\vec{\lambda}_i \cdot \vec{\lambda}_j}{4} \left[ \frac{1}{r_{ij}} - \frac{\pi \delta(\vec{r})}{m_i m_j} \left( 1 + \frac{2}{3} \vec{\sigma}_i \cdot \vec{\sigma}_j \right) \right], \quad (10)$$

where  $\vec{\lambda}(\vec{\sigma})$  is the  $SU_3^c$  Gell-Mann ( $SU_2^G$  Pauli) operator,  $\vec{r} = \vec{r}_i - \vec{r}_j$  and the other symbols have their usual meaning. Momentum dependent and tensor interactions are neglected in this calculation.  $V_{ij}^G$  is the Fermi-Breit approximation to single gluon exchange and the color screened confining interaction is defined by

$$V_{ij}^c = a_c \vec{\lambda}_i \cdot \vec{\lambda}_j \begin{cases} r & \text{if } i, j \text{ occur in the same baryon orbit,} \\ \frac{1-e^{-\kappa r}}{\kappa} & \text{if } i, j \text{ occur in different baryon orbits,} \end{cases} \quad (11)$$

Explicitly, eq.(11) means we use the non-screened, color-confinement potential, namely linear confinement, to calculate matrix elements  $\langle LL|V|LL \rangle$ ,  $\langle RR|V|RR \rangle$ ,  $\langle LL|V|RR \rangle$  and  $\langle RR|V|LL \rangle$ , and use the color-screening confinement potential to calculate the other matrix elements, such as  $\langle LR|V|LR \rangle$ ,  $\langle LL|V|LR \rangle$ . Here  $\langle LL|V|LL \rangle = \langle \phi_L(i)\phi_L(j)|V_{ij}|\phi_L(i)\phi_L(j) \rangle$ , etc.

For  $\langle LR|V|LR \rangle$ , the interacting quarks are clearly always in different baryons and so screened at longer distances. For  $\langle LL|V|LR \rangle$ , which form applies is not obvious and a model choice must be made. One could consider other choices such as an average of the two confinement forms. Another ambiguity occurs for  $s = 0$ , where we have only one baryon orbit. We define the matrix elements at  $s = 0$  to be the limit of the values as  $s$  tends to zero. Both of these model choices are consistent. We recognize that making these additional assumptions means that we no longer have simply a potential model but rather that we are implicitly including an approximation to many-body, low energy QCD interactions which cannot be included in two body confinement and Fermi-Breit interactions. (A similar inclusion occurs in models such as the "flip-flop" model. [13]) In

this sense, we are extending an effective matrix element method from bound states to scattering states.

A good feature of this model Hamiltonian is that it reduces to the usual non-screening, color-confinement model Hamiltonian for a single hadron and for two hadrons in the asymptotic region but the spurious color van der Waals force have been eliminated. The historical triumphs of the constituent quark model in explaining hadron spectroscopy are retained and the model parameters  $m$  ( $u, d$  quark mass),  $\alpha_s$  (quark-gluon coupling constant),  $a_c$  (strength of the confinement potential) and  $b$  (baryon size parameter) can be determined by the nucleon mass,  $N - \Delta$  mass splitting, and the stability condition for nucleon size,  $\partial M_N(b)/\partial b = 0$ , along with the usual choice,  $m = M_N/3$ . The  $s$  quark mass ( $m_s$ ) is most accurately determined by the difference of  $\Lambda$  and  $\Sigma$  masses.

The color screening constant  $\kappa$  is directly taken from lattice QCD results [6] and this is the reason for our having chosen a linear confinement and exponential color screening in this calculation even though quadratic confinement may be more proper for a nonrelativistic model [10]. The parameters fixed in this way are:

$$\begin{aligned} m &= 313 \text{ MeV}, m_s = 521.7 \text{ MeV}, b = 0.625 \text{ fm}, \\ \alpha_s &= 1.71, a_c = 39.1 \text{ MeV fm}^{-1}, \kappa = 1.1111 \text{ fm}^{-1} \end{aligned} \quad (12)$$

Note that the  $\Lambda$  and  $\Sigma$  masses calculated are 1025 MeV and 1103 MeV, 90 MeV lower than experimental values.

### III. CALCULATION METHOD

Due to delocalization, our GCM basis WF, eq.(1), includes not only the usual  $q^3$ - $q^3$  clustering, but also  $q^6$ ,  $q^5$ - $q$  and  $q^4$ - $q^2$  clustering, and therefore can not be factorized into internal, relative and center of mass WF in the interaction region. The usual cluster model method has to be extended [14]. Suppose  $\Psi$  is a solution of our model Hamiltonian eq.(9),

$$(H - E)\Psi = 0. \quad (13)$$

In general, both local and nonlocal interactions are included in  $H$ , but the nonlocal interaction is nonzero only within a limited interaction region  $r < a$ , where  $a$  is roughly determined by the scale at which the overlap of different orbitals, Eqs.(7) and (8), becomes negligible, and  $r$  refers here to the separation between two three-quark clusters (see Eq.(21) below). If we separate the whole space into interaction and asymptotic regions, then in the interaction region, we can rewrite eq.(13) as,

$$(H + \mathcal{L} - E)\Psi = \mathcal{L}\Psi, \quad (14)$$

where  $\mathcal{L}$  is the Bloch operator [15], which was introduced by Bloch to make the Hamiltonian Hermitian in a finite space. Taking the Hermitian conjugate of eq.(14) and using  $H^\dagger + \mathcal{L}^\dagger = H + \mathcal{L}$ , we obtain

$$\langle \Psi | H - E | \Psi_t \rangle |_0^a = \langle \Psi | \mathcal{L}^\dagger - \mathcal{L} | \Psi_t \rangle |_0^a. \quad (15)$$

where the notation  $|_0^a$  is intended to convey that the integration in  $r$  is restricted to  $0 < r < a$  and  $\Psi_t$  is a trial WF. Then a variational functional,  $J(\Psi_t)|_0^a$ , can be defined in the interaction region as,

$$\begin{aligned} J(\Psi_t)|_0^a &= \langle \Psi_t | H - E | \Psi_t \rangle |_0^a - \langle \Psi | H - E | \Psi_t \rangle |_0^a \\ &= \langle \Psi_t | H - E | \Psi_t \rangle |_0^\infty - \langle \Psi_t | H - E | \Psi_t \rangle |_a^\infty - \langle \Psi | \mathcal{L}^\dagger - \mathcal{L} | \Psi_t \rangle |_0^a, \end{aligned} \quad (16)$$

and this functional does have a variational minimum with respect to variation of the trial WF,  $\Psi_t$ . This can be seen from the fact that the first line is quadratic in the difference between the trial and exact WFs since, due to eq.(13),

$\langle \Psi_t | H - E | \Psi \rangle |_0^a = \langle \Psi | H - E | \Psi \rangle |_0^a = 0$ . The second line simply involves rewriting the first term in terms of the full and exterior ranges, and the second term has had the substitution made from eq.(15).

The GCM WF is written as

$$\Psi_t^{GCM} = \int f(\vec{s}) \Psi(\vec{s}) d\vec{s}, \quad (17)$$

where  $\Psi(\vec{s})$  is the six quark WF of eq.(1). Upon substituting this trial WF in eq.(16) and doing a partial wave decomposition (Only central interactions are studied here; if non-central interactions are to be included, this partial wave decomposition would have to be extended correspondingly.), we obtain

$$J_l(\Psi_t)|_0^a = \int ds ds' f_l(s) f_l(s') \widetilde{K}_l^{GCM}(s, s') - \mathcal{L}_l(a), \quad (18)$$

where

$$\widetilde{K}_l^{GCM}(s, s') = K_l^{GCM}(s, s') - K_l'^{GCM}(s, s'), \quad (19)$$

$$\frac{K_l^{GCM}(s, s')}{ss'} = \int Y_{lm}^*(\hat{s}) \langle \Psi(\vec{s}) | H - E | \Psi(\vec{s}') \rangle Y_{lm}(\hat{s}') d\hat{s} d\hat{s}', \quad (20)$$

$$K_l'^{GCM}(s, s') = c_l \int_a^\infty dr \Gamma_l(r, s) \left[ -\frac{\hbar^2}{2\mu} \left( \frac{d^2}{dr^2} - \frac{l(l+1)}{r^2} \right) + V^c(r) - E_r \right] \Gamma_l(r, s') \quad (21)$$

where here,  $\vec{r} = (\frac{\vec{r}_4 + \vec{r}_5 + \vec{r}_6}{3} - \frac{\vec{r}_1 + \vec{r}_2 + \vec{r}_3}{3})$ ,  $c_l = 1 - (-)^{S+T+l} \delta_{AB}$ , and  $E_r$  is the energy of relative motion.

To obtain eq.(21), we have assumed that, in the asymptotic region: All of the exchange color interactions have died out; only the long range Coulomb interaction,  $V^c(r)$ , for charged baryons may remain; the delocalization has disappeared ( $\epsilon = 0$ ); and the six quark system has clustered into two three quark baryons  $A$  and  $B$ .

$\Gamma_l(r, s)$  is the  $l$ th partial wave of the relative motion WF,  $\Gamma(\vec{r}, \vec{s})$ , obtained from the WF of eq.(1) when it is factorized into internal, relative and center of mass parts of two three quark clusters (see eq.(32) below).

$$\Gamma(\vec{r}, \vec{s}) = \left( \frac{3}{2\pi b^2} \right)^{3/4} e^{-\frac{3}{4b^2}(\vec{r}-\vec{s})^2}, \quad (22)$$

$$\Gamma_l(r, s) = \left( \frac{3}{2\pi b^2} \right)^{3/4} e^{-\frac{3}{4b^2}(r^2+s^2)} 4\pi r s i^l j_l(-i \frac{3}{2b^2} r s). \quad (23)$$

Finally

$$\mathcal{L}_l(a) = (c_l \frac{\hbar^2}{2\mu}) \left[ g_l'(a)g_l^t(a) - g_l(a)g_l'^t(a) \right]. \quad (24)$$

$$g_l^t(r) = \int f_l(s) \Gamma_l(r, s) ds, \quad (25)$$

and  $g_l(r)$  is the radial part of the relative motion WF of the exact solution  $\Psi$  of eq.(13).

The Bloch operator  $\mathcal{L} = \frac{\hbar^2}{2\mu} \frac{1}{a} \delta(r - a) \frac{d}{dr} r$  has been used in deriving eq.(24).

Next we follow Canto and Brink [16], assuming as a boundary condition that the trial and exact logarithmic derivatives are equal at the boundary,

$$L_l^t = \frac{g_l'^t(a)}{g_l^t(a)} = L_l = \frac{g_l'(a)}{g_l(a)}. \quad (26)$$

This implies that  $\mathcal{L}_l(a) = 0$ .

Making use of the stability property of the functional  $J(\Psi^t)$ , we vary  $J(\Psi^t)$  with respect to the trial WF  $f_l(r)$  to obtain the equation of motion of  $f_l(r)$ . The advantage of the Canto-Brink variational method is that one need not solve this equation of motion, but that instead one can obtain the logarithmic derivative  $L_l^t$  directly via

$$L_l^t = \frac{1}{\sum_{i,j} \Gamma_l(a, s_i) Q_{ij}^{-1} \Gamma_l(a, s_j)} \quad (27)$$

$$Q_{ij} = \frac{2\mu}{\hbar^2} \frac{K_{ij}}{c_l} - \int_a^\infty dr \left[ \frac{d}{dr} \Gamma_l(r, s_i) \frac{d}{dr} \Gamma_l(r, s_j) + \Gamma_l(r, s_i) w(r) \Gamma_l(r, s_j) \right], \quad (28)$$

$$K_{ij} = K_l^{GCM}(s_i, s_j)$$

$$w(r) = \frac{l(l+1)}{r^2} + \frac{2\mu}{\hbar^2} [V^c(r) - E_r].$$

Phase shifts can then be obtained through  $L_l^t$ ,

$$\delta_l = \tan^{-1} \left[ \frac{kF_l'(ka) - L_l^t F_l(ka)}{L_l^t G_l(ka) - kG_l'(ka)} \right], \quad (29)$$

where  $F$  and  $G$  are Coulomb WFs.

The difference between our derivation and that of Canto and Brink is that we do not assume that the trial WF basis,  $\Psi$  of eq.(1), can be factorized into the internal, relative and center of mass parts in the interaction region. In fact, it is impossible to do so for our delocalized WF.

The main task remaining is to calculate the GCM kernel  $K^{GCM}(\vec{s}, \vec{s}')$ . The color part is standard. The spin-isospin part is also unaltered for the N-N channel, but different from that of others [17] for the N- $\Lambda$  and N- $\Sigma$  channels because we use a spin-flavor asymmetric hyperon WF and the antisymmetrization is restricted within the five  $u, d$  quarks. The orbital matrix elements are more involved due to delocalization; in particular, the center of mass motion must be properly eliminated. We use a momentum projection method to project out the  $\vec{P}_c = 0$  part,

$$\frac{1}{\sqrt{V}} \int d\vec{r}_c e^{-i\vec{P}_c \cdot \vec{r}_c} \Psi(\vec{r}_1, \dots, \vec{r}_6). \quad (30)$$

As mentioned before, our GCM basis WF includes not only  $l^3 r^3$ , but also  $l^6 r^0$ ,  $l^5 r^1$ ,  $l^4 r^2$ ,  $l^2 r^4$ ,  $l^1 r^5$ ,  $l^0 r^6$  configurations. Here  $l^{n_1} r^{n_2}$  means,

$$\prod_{i=1}^{n_1} \phi_L(\vec{r}_i - \vec{s}_1) \prod_{j=n_1+1}^{n_1+n_2} \phi_R(\vec{r}_j - \vec{s}_2) \quad (31)$$

which can be factorized to the form

$$\Phi_{B_1}(\xi_1) \Phi_{B_2}(\xi_2) \exp \left\{ -\frac{1}{2b^2} \left[ \frac{n_1 n_2}{n} (\vec{r} - \vec{s})^2 + n(\vec{r}_c - \vec{s}_c)^2 \right] \right\}, \quad (32)$$

where

$$\begin{aligned} \vec{r} &= \vec{R}_2 - \vec{R}_1, & \vec{s} &= \vec{s}_2 - \vec{s}_1, \\ \vec{r}_c &= \frac{n_1 \vec{R}_1 + n_2 \vec{R}_2}{n} = \frac{\sum_{i=1}^n \vec{r}_i}{n}, & \vec{s}_c &= \frac{n_1 \vec{s}_1 + n_2 \vec{s}_2}{n}, \\ \vec{R}_1 &= \frac{\sum_{i=1}^{n_1} \vec{r}_i}{n_1}, & \vec{R}_2 &= \frac{\sum_{j=n_1+1}^n \vec{r}_j}{n_2}, \end{aligned} \quad (33)$$

(34)

and  $\xi_1(\xi_2)$  are the internal coordinates of the  $n_1(n_2)$  quark cluster.

Different configurations have different  $\vec{s}_c$ , but the same  $\vec{r}_c = (\sum_{i=1}^n \vec{r}_i)/n$ . Let us introduce the parameter center  $\vec{t} = (\vec{s}_1 + \vec{s}_2)/2$ . Then  $\vec{s}_c = \vec{t} - (3-i)\vec{s}/6$ , where  $i = 0, 1, \dots, 6$  corresponds to the  $(n_1, n_2) = (6, 0), (5, 1), (4, 2), (3, 3), (2, 4), (1, 5), (0, 6)$  particle partitions. (This result can obviously be extended to any N-particle system.) By means of  $\vec{t}$  and  $\vec{s}$ , the exponential part of eq.(32) can be written as

$$\exp \left\{ -\frac{1}{2b^2} \left[ \frac{n_1 n_2}{n} (\vec{r} - \vec{s})^2 + n(\vec{r}_c - \vec{t})^2 + n \frac{(3-i)^2}{36} s^2 + \frac{n(3-i)}{3} (\vec{r}_c - \vec{t}) \cdot \vec{s} \right] \right\}. \quad (35)$$

Due to the appearance of  $\vec{r}_c$  only in the combination  $(\vec{r}_c - \vec{t})$  in eq.(35), the momentum projection, eq.(30), can be written as

$$\frac{1}{\sqrt{V}} \int d\vec{r}_c e^{-i\vec{P}_c \cdot \vec{r}_c} \Psi(\vec{r}_1, \dots, \vec{r}_6) = \frac{1}{\sqrt{V}} \int d\vec{t} e^{-i\vec{P}_c \cdot \vec{t}} \Psi(\vec{r}_1, \dots, \vec{r}_6) \xrightarrow{\vec{P}_c=0} \frac{1}{\sqrt{V}} \int d\vec{t} \Psi(\vec{r}_1, \dots, \vec{r}_6) \quad (36)$$

The spurious center of mass motion part of the GCM kernel can thus be eliminated by a double momentum projection

$$\frac{1}{V} \int d\vec{t} d\vec{t}' \langle \Psi(\vec{s}) | H - E | \Psi(\vec{s}') \rangle. \quad (37)$$

When we used this momentum projection method to calculate the matrix elements of the kinetic energy and the Galilean noninvariant Darwin term of the one gluon exchange Fermi-Breit interaction, we obtained the same analytic formulas as those of Fujiwara [3]. Our variational method has been checked with Fujiwara's numerical results [3] as well.

#### IV. RESULTS

Initially, we carried out a unified, parameter free (i.e., all parameters are determined by single hadron properties and the color screening constant is taken from lattice QCD,) model calculation of the N-N, N- $\Lambda$  and N- $\Sigma$  interactions. This was done to check whether the quarks delocalize reasonably in the different flavor channels to give rise to qualitatively correct N-N, N- $\Lambda$  and N- $\Sigma$  effective interactions. These effective interactions are shown in figs.1-3 ( $NN$   $ST = 01, 10$ ;  $N\Lambda$   $ST = 0\frac{1}{2}, 1\frac{1}{2}$ ,  $N\Sigma$   $ST = 0\frac{1}{2}, 1\frac{1}{2}, 0\frac{3}{2}, 1\frac{3}{2}$ ) and indeed qualitatively reproduce the phenomenological results. That is, the intermediate range attractions, usually assumed to be due to meson exchange, are reproduced by the quark delocalization in the QDCSM. In the N-N channels, this model even gives rise to semi-quantitatively correct effective interactions; figs.4-5 show the  $^1S_0, ^3S_1$  and  $^1D_2$  N-N phase shift fits. [21]

Figs.2-3 shows the results for  $N-\Sigma$  and  $N-\Lambda$  channels. For  $N-\Lambda$ , the spin triplet state is somewhat more attractive than the spin singlet; channel coupling adds a bit more attraction to this state but leaves the spin singlet almost unchanged. We note that  $^4H$  and  $^4He$  both have spin zero ground states and spin one excited states. One might interpret this as evidence that the spin-singlet  $N-\Lambda$  interaction is more attractive than the spin triplet. However, the situation is not so transparent due to the complications of the interactions of the four bodies involved and, in addition,  $\Lambda-\Sigma^0$  mixing effects. The spin one ground state of the deuteron is certainly an indication that the spin triplet  $N-N$  interaction is more attractive than the spin triplet, and we might reasonably expect (by flavor symmetry) that this should hold true for all octet-baryon combinations. However, due to the strong tensor interaction from pion exchange, the Nijmegen OBE model F [1] nonetheless includes a more attractive spin singlet  $N-N$  central interaction. Furthermore, there is a paucity of direct data on scattering in the  $Y-N$  channels, and widely differing relative strengths for the central interaction are all consistent with both the available data and the nuclear states referred to above. The QDCSM, on the other hand, predicts that spin triplet  $N-N$  and  $N-\Lambda$  interactions are stronger than spin singlet ones. Clearly, which central interaction is stronger in each case merits additional study.

For  $N-\Sigma$ , we find the strongest attraction in the  $IJ = \frac{1}{2}1$  channel, while the  $IJ = \frac{3}{2}0$ , and  $\frac{1}{2}0$  channels both have a little weaker attraction (single channel case), and the  $IJ = \frac{3}{2}1$  channel is repulsive. Channel coupling has little effect on  $\frac{1}{2}1$ , and pushes  $\frac{1}{2}0$  from attractive to repulsive. These show that the  $N-\Sigma$  potential is more strongly spin and/or isospin dependent than the  $N-\Lambda$  potentials, which have a little weaker dependence on spin. These results are in qualitative agreement with the calculations of OBE models [1,2] and hybrid quark model calculations [3], except that our attraction for the  $N-\Sigma(\frac{1}{2}1)$  channel is too strong.

To check if one can obtain a semi-quantitative fit of  $N-\Lambda$  and  $N-\Sigma$  scattering by fine tuning of the model parameters, two kinds of adjustment of the color screening parameter,  $\kappa$ , have been made: The first keeps the color screening parameter  $\kappa$  for the  $u, d$  quarks unchanged, i.e.,  $\kappa_u = \kappa_d = 1.11\text{fm}^{-1}$ , but allows  $\kappa_s$  for the  $s$ -quark to vary; the second one keeps  $\kappa_u = \kappa_d = \kappa_s = \kappa$  but allows the value of  $\kappa$  to vary for the  $N-\Lambda$  and  $N-\Sigma$  channels.

Figs.6, 7 and 8 show phase shifts for the  $N\Lambda$   $ST = 0\frac{1}{2}, 1\frac{1}{2}$  and  $N\Sigma$   $ST = 0\frac{1}{2}, 1\frac{1}{2}$  and  $0\frac{3}{2}, 1\frac{3}{2}$  channels with  $\kappa_s = \frac{4}{9}\kappa_u$ . These are similar, but not identical to other hybrid quark model

results [3,18]. Figs.9, 10, 11, 12 and 13 show integral and differential scattering cross sections [22,23] for  $N\Lambda$ ,  $p\Sigma^+$  and  $p\Sigma^-$ . A qualitative fit is obtained even though our model phase shifts differ from others. This feature occurs in the meson exchange model as well; the Nijmegen models D and F [1] also have quite different phase shifts from each other. Quantitatively, the  $N\Lambda$  total cross section is fit quite well. [22] We have shown that channel coupling does not change the  $N\Lambda$  interaction very much; therefore, this good fit will be maintained even after  $N\Lambda$  and  $N\Sigma$  channel couplings are taken into account. The  $p\Sigma^+$  cross section found in the model is larger than the experimental value [23] and this channel does not couple to any others. Hence, some fine-tuning may be needed. Conversely, the  $p\Sigma^-$  cross section found in the model is smaller than the experimental value. [23] For that case, a channel coupling calculation is needed to determine if the fit can be improved by strong channel coupling effects.

## V. CONCLUSION

The QDCSM has been used to calculate the effective  $N\Lambda$ ,  $N\Sigma$  and  $N\Lambda$  interactions. Linear confinement, with a color screening constant taking from lattice QCD, has been used in this calculation. All other model parameters are determined from the properties of baryons. This means that we have a parameter-free model calculation for nucleon-baryon (N-B) interactions. We find that the quarks delocalize reasonably in the different flavor channels (10 altogether) to induce qualitatively correct, effective N-B interactions except that the  $N\Lambda$  (1/2,1) and  $N\Sigma$  (1/2,1) channels have attractions that are somewhat too strong. For the  $N\Lambda$  channels, this model even gives semi-quantitatively correct phase shifts in the  $^1S_0$ ,  $^3S_1$ , and  $^1D_2$  partial waves. After fine tuning the color screening constant, we find it also gives semi-quantitatively correct scattering cross sections for the  $N\Lambda$  and  $N\Sigma$  channels.

Several points need to be improved upon and to be checked further.

- 1. So far, only single channel dynamical calculations have been done. The effect of dynamical channel coupling must be checked, especially for the  $N\Sigma$  channel.
- 2. Only central interactions have been included in this calculation. Non-central interactions need to be studied and higher partial wave scattering should be checked correspondingly.
- 3. A better fit of the existing N-B scattering data better would support the QDCSM, but achieving such an improvement is not be the primary goal of this model calculation. In fact, nucleon-hyperon scattering data is so sparse that different meson exchange models fit the data perfectly well, and hybrid quark models can be made to fit the data as well, if one is willing to fine tune as has been done for meson exchange models. Since the fundamental strong interaction theory is certainly QCD, the N-B interactions should be an excellent area in which to study non-perturbative QCD. Meson-baryon and quark-gluon descriptions both are able to describe the N-B interactions if we are willing to include the whole hierarchy of meson and baryon excited states and the totality of quark-gluon interaction diagrams [19]. However, we

may well ask which one is the most economical approach for including major non-perturbative QCD effects and for paving the way to new strong interaction physics such as exotic quark-gluon states, strangelets and so on. That the QDCSM obtains a qualitative, and in some cases, even a semi-quantitative, fit to N-B scattering and few nucleon systems <sup>[10]</sup> in its very naive version, might be an indication that it includes a substantial component of the true physics. The QCD basis of its model Hamiltonian needs to be studied further.

- 4. Nucleon spin structure studies show that the pure valence constituent quark model is only a first approximation. However, quark-antiquark excitation Fock components are certainly present in the ground state of the nucleon <sup>[20]</sup>. This fact should be taken into account in any quark model approach to hadron structure and hadron interaction studies; the QDCSM also needs to be elaborated to include it.

This research is supported in part by the Department of Energy under contract W-7405-ENG-36 and in part by the NSF of China.

## REFERENCES

- [1] J.J.de Swart, P.M.M. Maessen and T.A. Rijken, in "Properties & Interactions of Hyperons", eds. B.F. Gibson, P.D. Barnes and K. Nakai, (World Scientific, Singapore, 1994), p.37 and references therein.
- [2] A.G. Reuber, *ibid.*, p.159 and references therein.
- [3] Y. Fujiwara, C. Nakamoto and Y. Suzuki, Phys. Rev. Lett. **76**, 2242 (1996) and references therein.
- [4] K. Saito, K. Tsushima and A. W. Thomas, Nucl. Phys. **A609**, 339 (1996).
- [5] P. LaFrance and E.L. Lomon, Phys. Rev. D **34**, 1341 (1986).
- [6] K.D. Born, E. Lacermann, N. Pirch, T.E. Walsh and P.M. Zerwas, Phys. Rev., D **40**, 1653 (1989).
- [7] W. Lucha, F.F. Schöberl and D. Gromes, Phys. Rep. **200**, 127 (1991).
- [8] A.J. Buchmann, G. Wagner and A. Faessler, Phys. Rev. C **57**, 3340 (1998).
- [9] A. Bohr and B.R. Mottelson, Nuclear Structure, Vol.I, (W.A. Benjamin, Inc., New York, 1965), p.269.
- [10] T. Goldman, in "Nuclear Chromodynamics", eds. S. Brodsky and E. Moniz, (World Scientific, Singapore, 1986), p.363.  
T. Goldman, K. Maltman, G.J. Stephenson, Jr. and K.E. Schmidt, Nucl. Phys. **A481**, 621 (1988).  
F. Wang, G.H. Wu L.J. Teng and T. Goldman, Phys. Rev. Lett. **69**, 2901 (1992).  
K. Maltman, G.J. Stephenson, Jr. and T. Goldman, Phys. Lett. **B324**, 1 (1994).  
F. Wang, J.L. Ping, G.H. Wu, L.J. Teng and T. Goldman, Phys. Rev. C **51**, 3411 (1995).  
G.H. Wu, L.J. Teng, J.L. Ping, F. Wang and T. Goldman, Phys. Rev. C **53**, 1161 (1996).  
T. Goldman, K. Maltman, G.J. Stephenson, Jr., J.L. Ping and F. Wang, Mod. Phys. Lett. **A13**, 59 (1997).
- [11] N. Isgur, in "Topical Conference on Nuclear Chromodynamics", eds. J. Qiu and D. Sivers, (World Scientific, Singapore, 1988), p.201.
- [12] C.W. Wong, Phys. Rev. C **57**, 1962 (1998).
- [13] F. Lenz, J.T. Londergan, E.J. Moniz, R. Rosenfelder, M. Stingl and K. Yazaki, Ann. Phys. **170**, 65 (1986).
- [14] G.H. Wu and D.L. Yang, Sci. Sinica, Supp. A, 1112 (1982).
- [15] C. Bloch, Nucl. Phys. **4**, 503 (1957).
- [16] L.F. Canto and D.M. Brink, Nucl. Phys. **A279**, 85 (1977).
- [17] M. Oka, K. Shimizu, and K. Yazaki, Nucl. Phys. **A464**, 700 (1987).
- [18] U. Straub, *et al.*, Nucl. Phys. **A483**, 686 (1988); **A508**, 385c (1990).
- [19] H. Hofestadt, S. Merk and H.R. Petry, Z. Phys. **A326**, 391 (1987).  
F. Wang, Prog. Phys. **9**, 297 (1989).  
F. Wang and C.W. Wong, in "Quark-Gluon Structure of Hadrons and Nuclei", eds. L.S. Kisslinger and X.J. Qiu (International Academic Press, London, 1991), p.100.  
R.L. Jaffe, Nucl. Phys. **A522**, 365c (1991).
- [20] D. Qing, X.S. Chen and F. Wang, Phys. Rev. C **57**, R31 (1998); Phys. Rev. D **58** (in press).

- [21] C. Oh, R.A. Arndt, I.I. Strakovsky and R.L. Workman, Phys. Rev. C **56**, 635 (1997); nucl-th/9702006; R.A. Arndt, J.S. Hyslop, III, and L. D. Roper, Phys. Rev. D **35**, 128 (1987); R.A. Arndt *et al.*, Phys. Rev. D **28**, 97 (1983).
- [22] G. Alexander, U. Karshon, A. Shapira, G. Yekutieli, R. Engelmann, H. Filthuth and W. Lughofer, Phys. Rev. **173**, 1452 (1968); B. Sechi-Zorn, B. Kehoe, I. Twitty and R.A. Burnstein, Phys. Rev. **175**, 1735 (1968); J.A. Kadyk, G. Alexander, J.H. Chan, P. Gaposchkin and G.H. Trilling, Nucl. Phys. **B27**, 13 (1971).
- [23] F. Eisele, H. Filthuth, W. Föhlish, V. Hepp and G. Zech, Phys. Lett. **B37**, 204 (1971).

## FIGURE CAPTIONS

Fig. 1 Effective potential in MeV vs. baryon separation in  $fm$  for  $N-N$  channels with confinement parameter value,  $\kappa = 1.111 fm^{-1}$ .

Fig. 2 Effective potential in MeV vs. baryon separation in  $fm$  for  $N-\Sigma$  channels with confinement parameter value,  $\kappa = 1.111 fm^{-1}$ .

Fig. 3 Effective potential in MeV vs. baryon separation in  $fm$  for  $N-\Lambda$  channels with confinement parameter value,  $\kappa = 1.111 fm^{-1}$ .

Fig. 4 Phase shifts in degrees vs. center of mass energy in MeV for  $^1S_0$  and  $^3S_1$   $N-N$  channels compared with data [21].

Fig. 5 Phase shifts in degrees vs. center of mass energy in MeV for  $^1D_2$   $N-N$  channel compared with data [21].

Fig. 6 Scattering phase shifts in degrees vs. center of mass energy in MeV for  $N-\Lambda$  channels with confinement parameter value,  $\kappa_s = \frac{4}{9}\kappa$ .

Fig. 7 Scattering phase shifts in degrees vs. center of mass energy in MeV for  $N-\Sigma$ ,  $T = 1/2$  channels with confinement parameter value,  $\kappa_s = \frac{4}{9}\kappa$ .

Fig. 8 Scattering phase shifts in degrees vs. center of mass energy in MeV for  $N-\Sigma$ ,  $T = 3/2$  channels with confinement parameter value,  $\kappa_s = \frac{4}{9}\kappa$ .

Fig. 9 Cross section in  $mb$  vs. incident nucleon laboratory momentum in  $MeV/c$  for  $N-\Lambda$  scattering, compared with data [22].

Fig. 10 Cross section in  $mb$  vs. incident nucleon laboratory momentum in  $MeV/c$  for  $p-\Sigma^-$  scattering, compared with data [23].

Fig. 11 Cross section in  $mb$  vs. incident nucleon laboratory momentum in  $MeV/c$  for  $p-\Sigma^+$  scattering, compared with data [23].

Fig. 12 Differential cross section in  $mb$  vs. cosine of center of mass scattering angle at incident  $\Sigma^-$  laboratory momentum of  $160 MeV/c$  for  $p-\Sigma^-$  scattering, compared with data [23].

Fig. 13 Differential cross section in  $mb$  vs. cosine of center of mass scattering angle at incident  $\Sigma^+$  laboratory momentum of  $170 MeV/c$  for  $p-\Sigma^+$  scattering, compared with data [23].

Fig.10  $p\Sigma^-$  Scattering Cross-sections

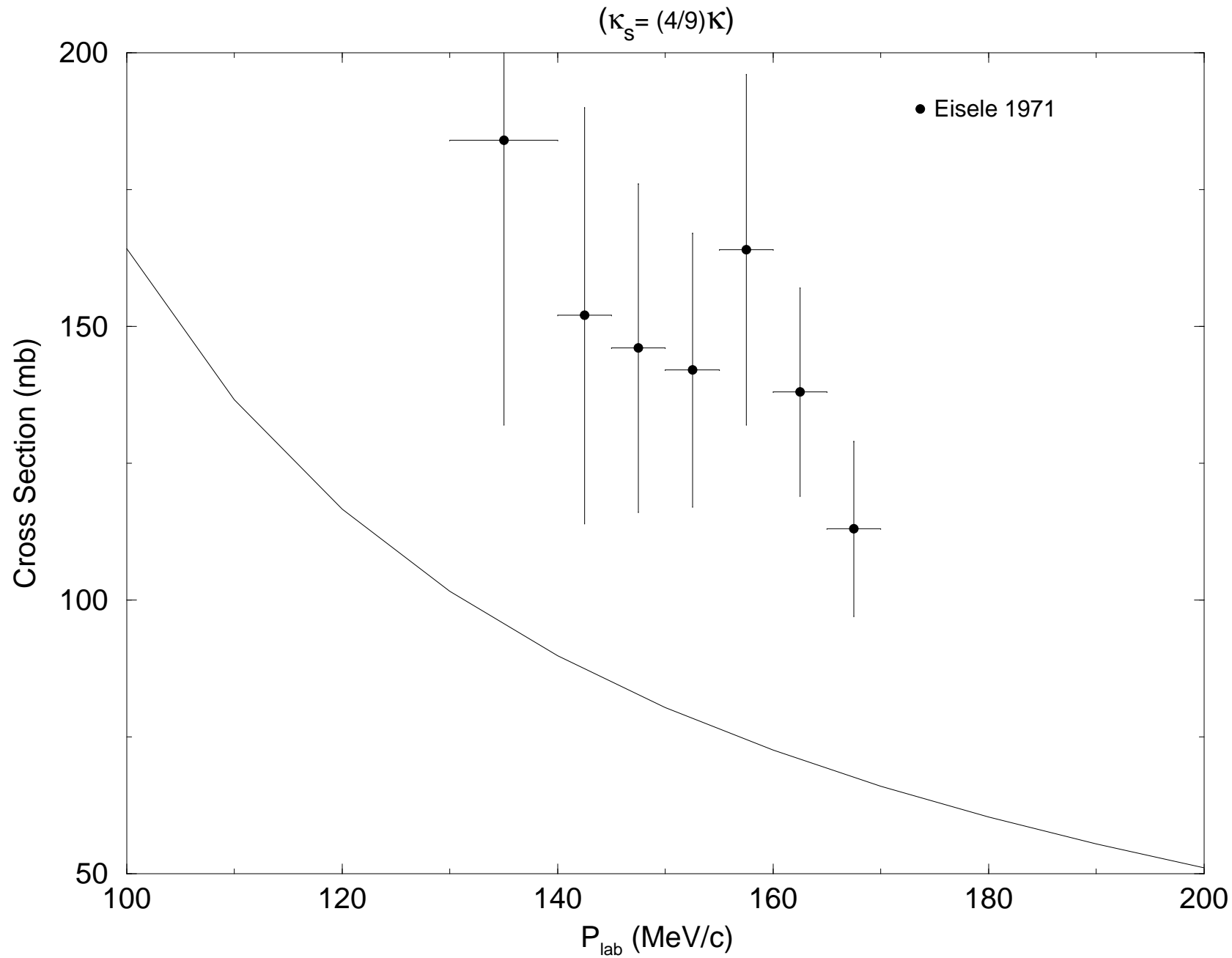


Fig.11  $p\Sigma^+$  Scattering Cross–sections

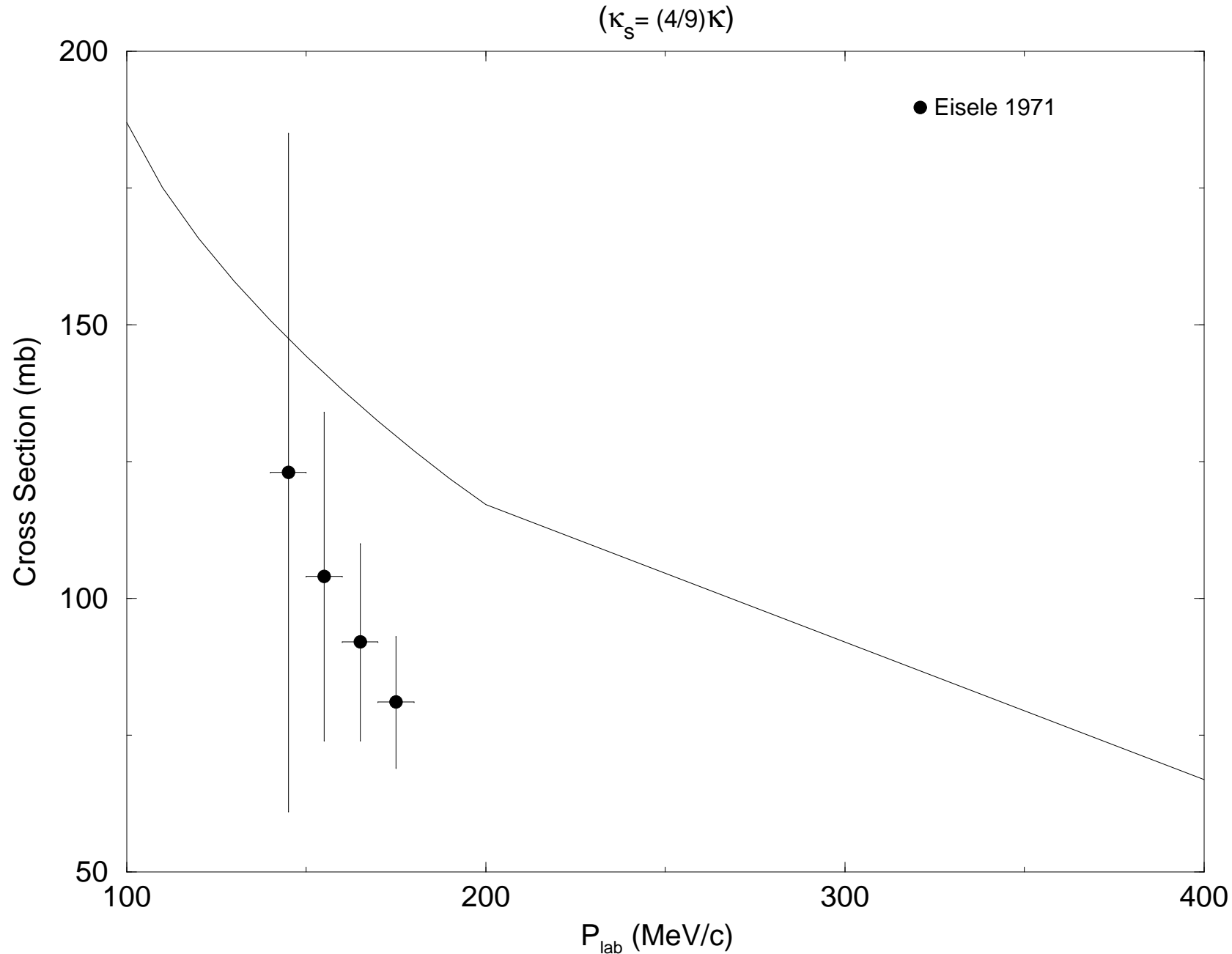


Fig.12  $p\Sigma^-$  Differential Cross-sections

$(\kappa_s = (4/9)\kappa)$

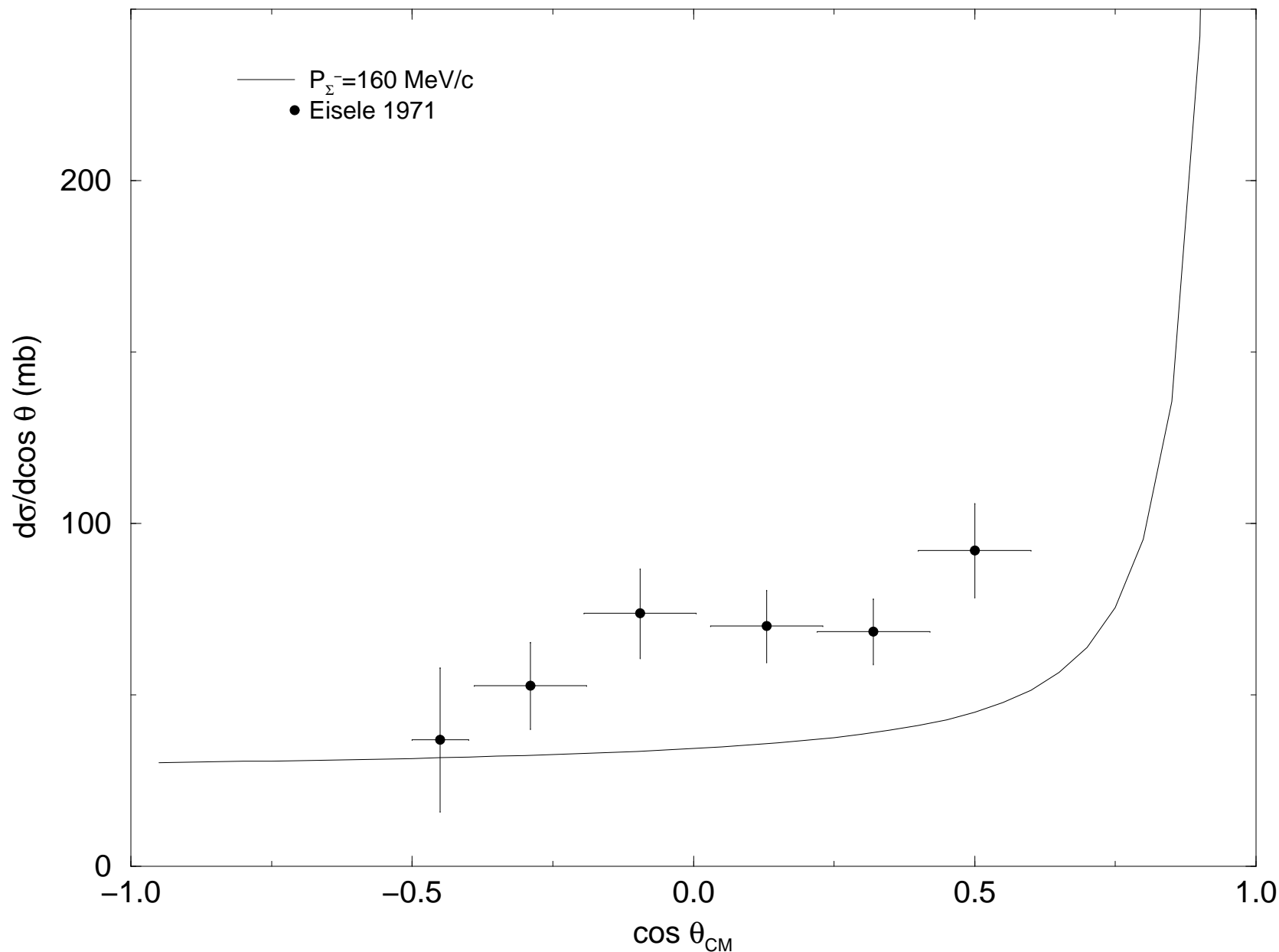


Fig.13  $p\Sigma^+$  Differential Cross-sections

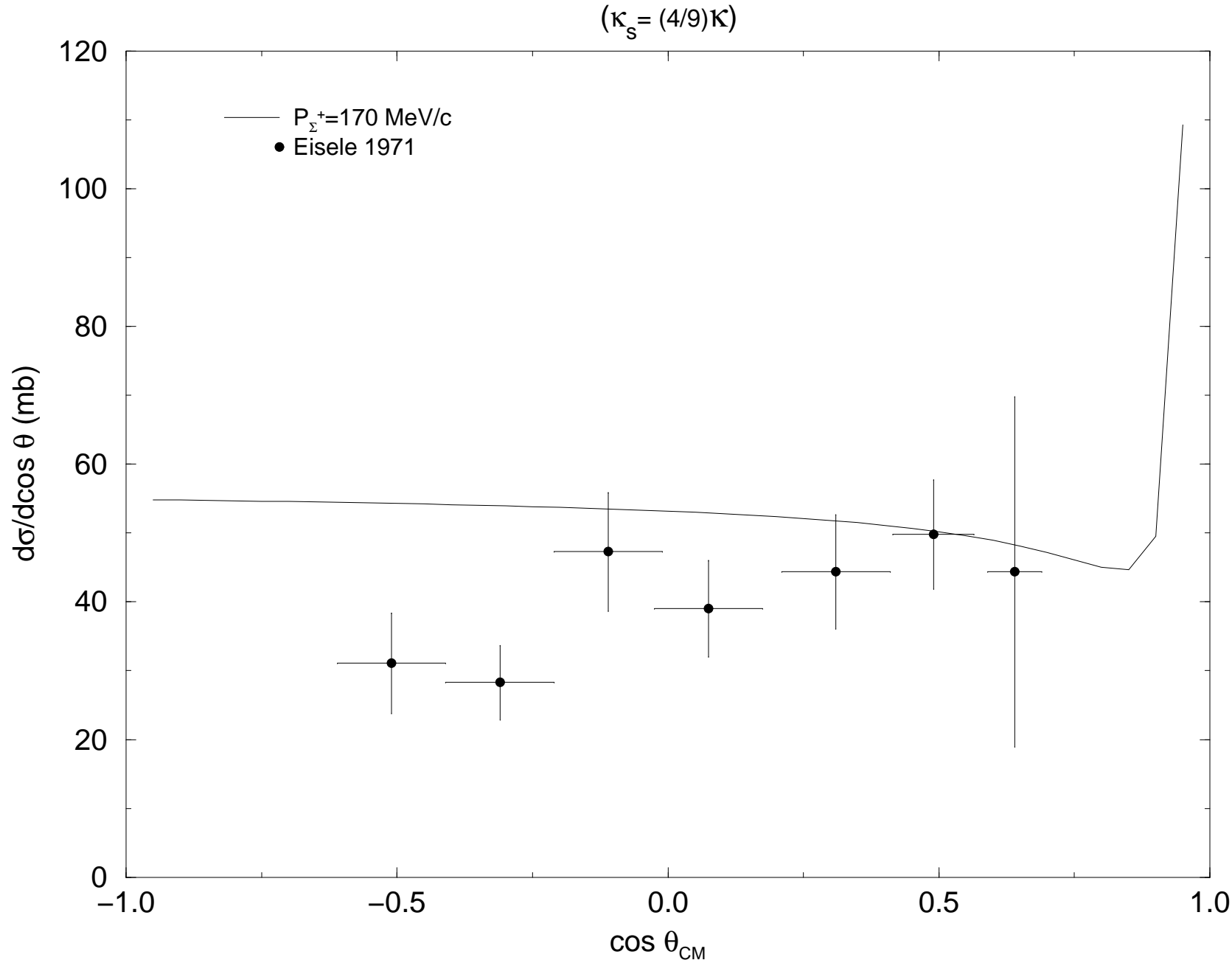


Fig.1 Effective potential

(for NN with  $\kappa=1.111 \text{ fm}^{-1}$ )

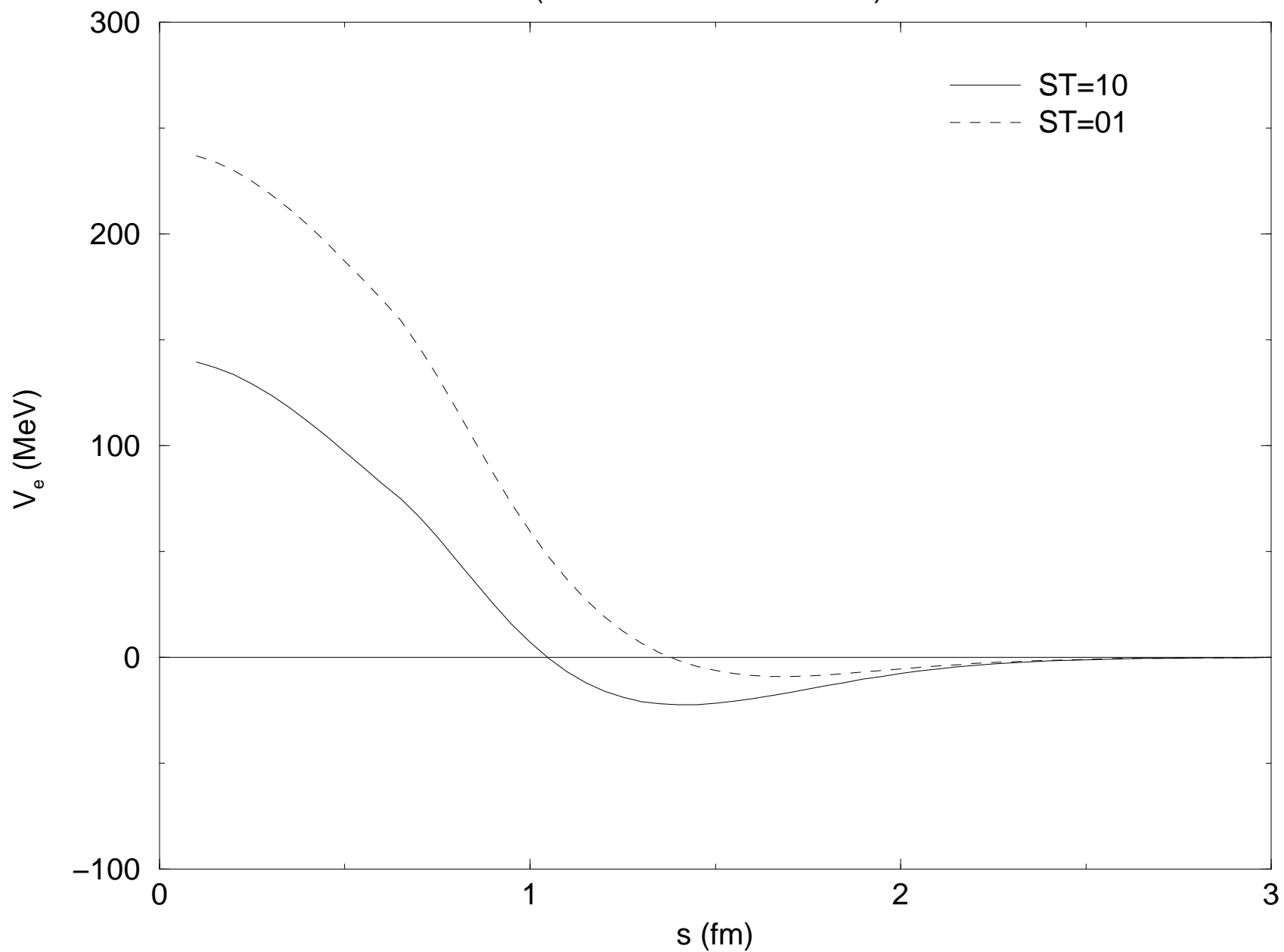


Fig.2. Effective potential

(for  $N\Sigma$  with  $\kappa=1.111 \text{ fm}^{-1}$ )

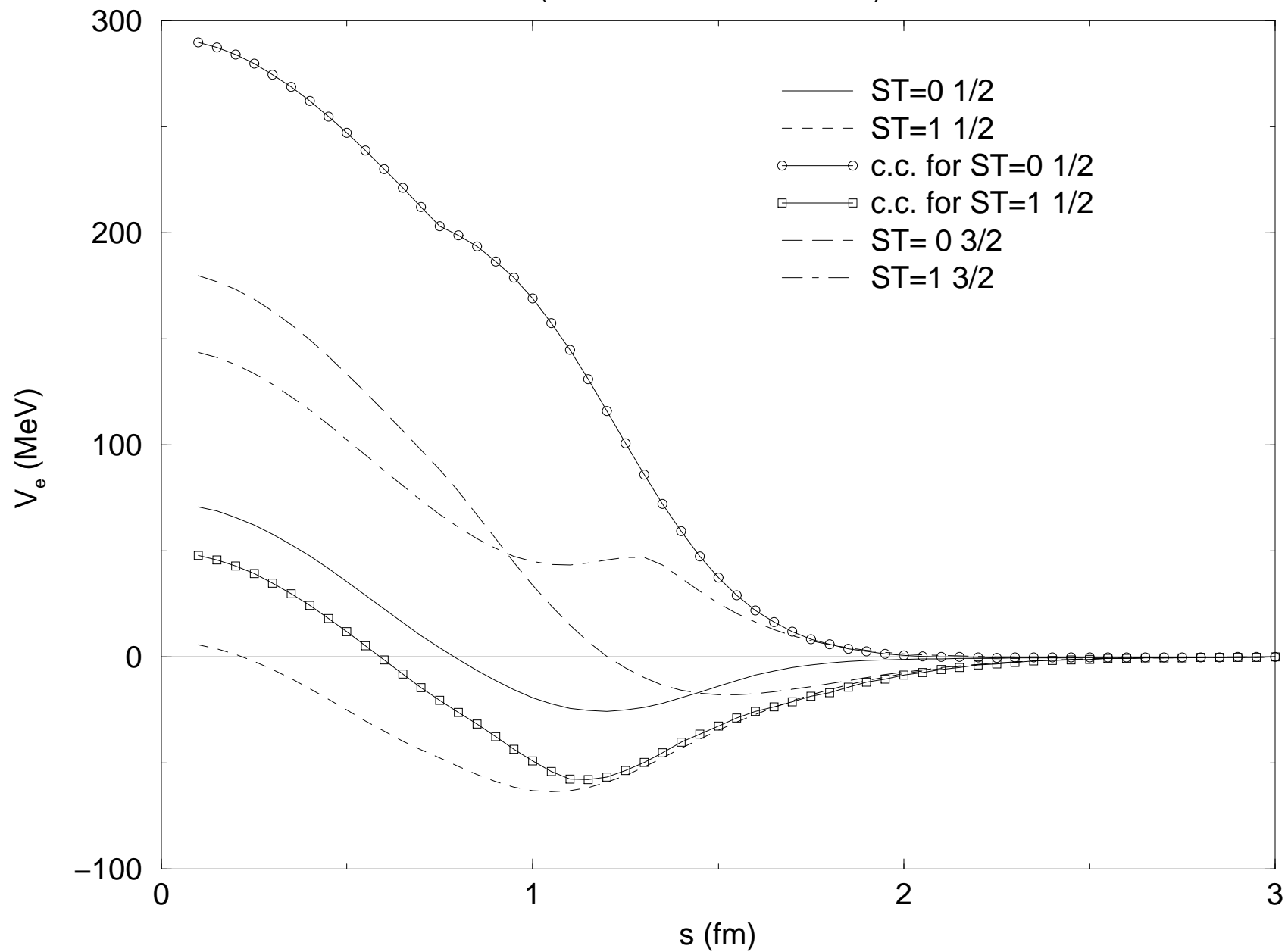


Fig.3. Effective potential

(for  $N\Lambda$  with  $\kappa=1.111 \text{ fm}^{-1}$ )

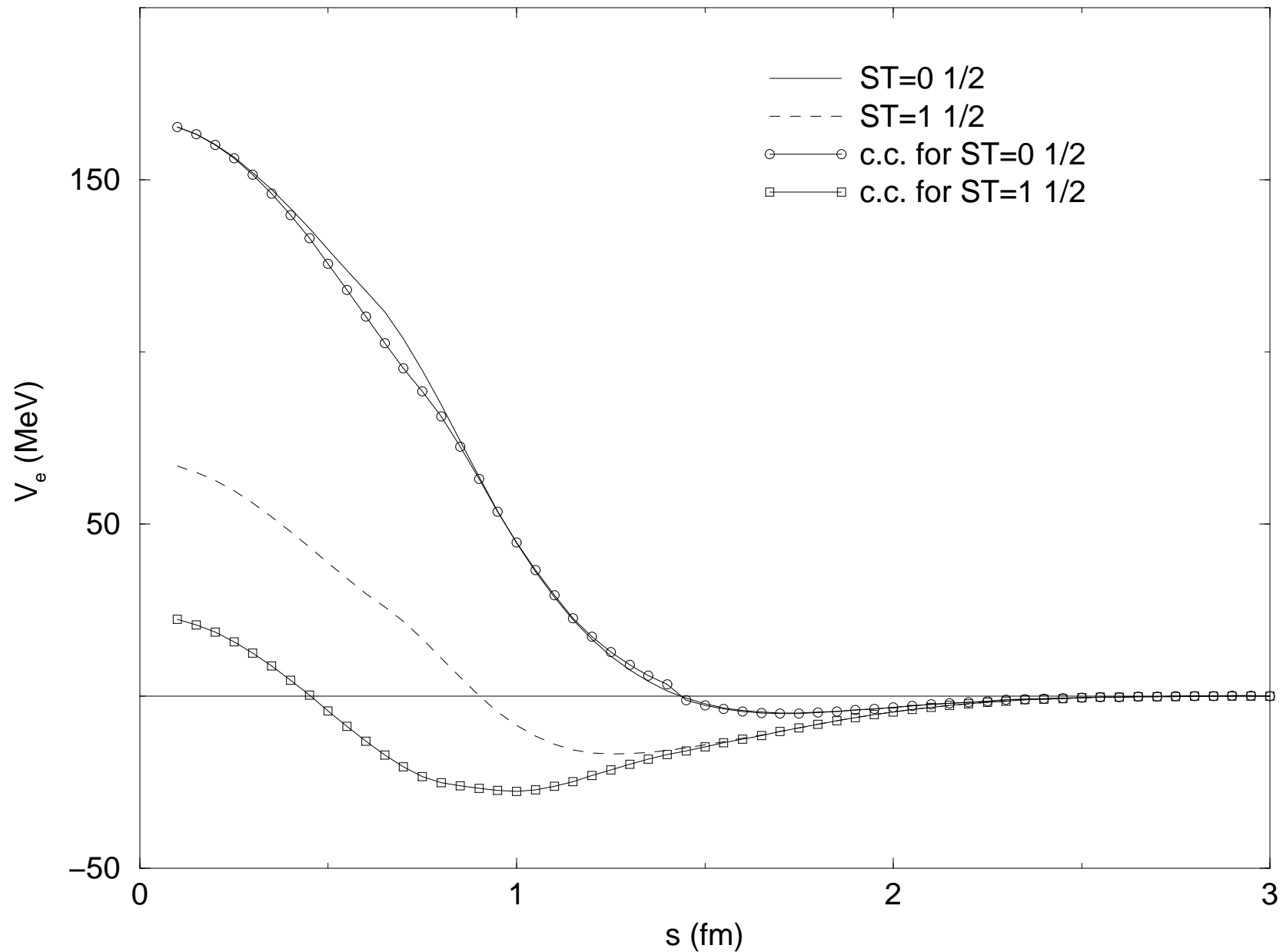


Fig.4 N–N  $^1S_0$  and  $^3S_1$  phase shifts  
 $(\kappa=1.111 \text{ fm}^{-1})$

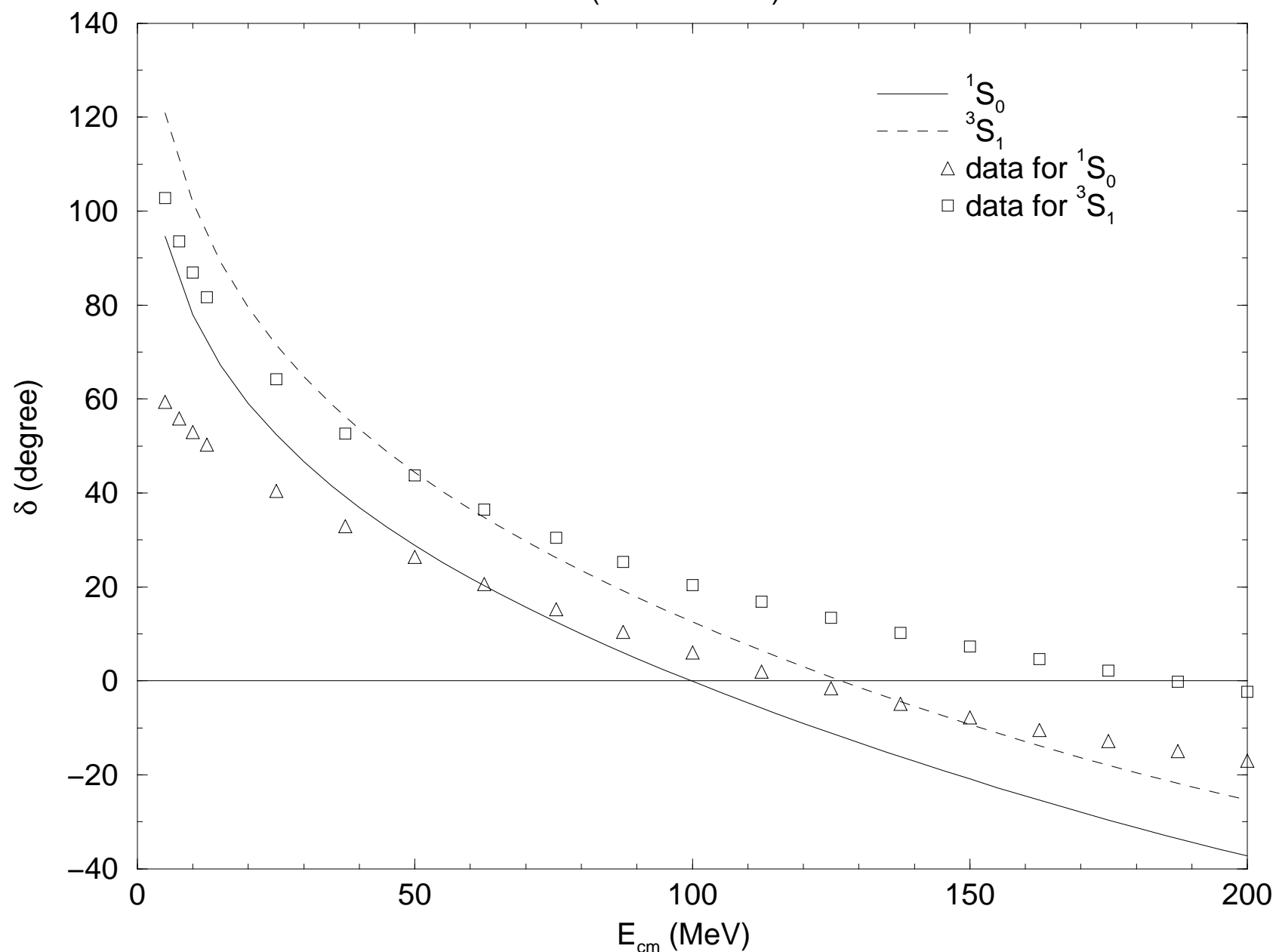
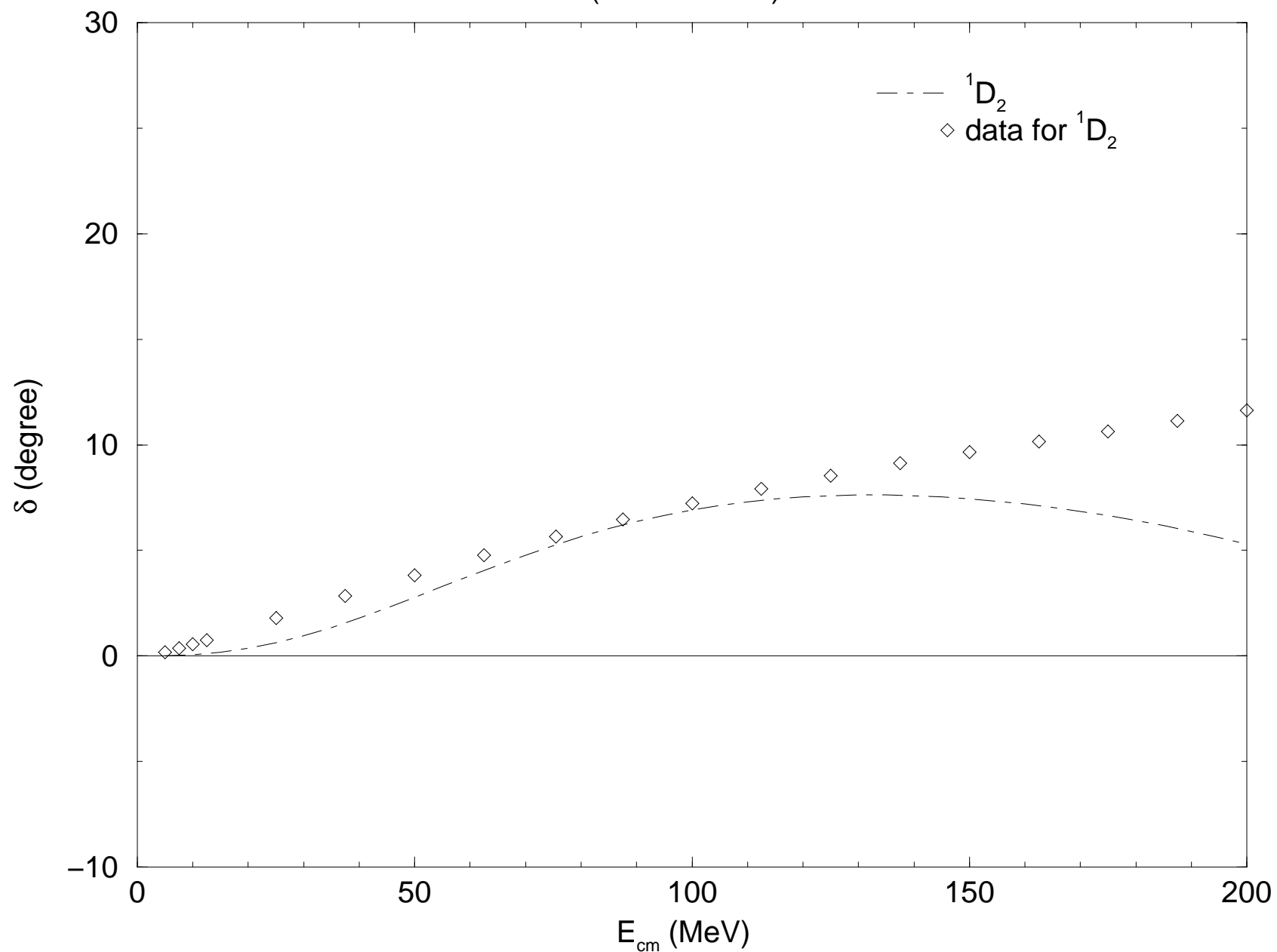


Fig.5 N–N  $^1\text{D}_2$  phase shifts

( $\kappa=1.111 \text{ fm}^{-1}$ )



# Fig.6 NΛ Scattering Phase Shifts

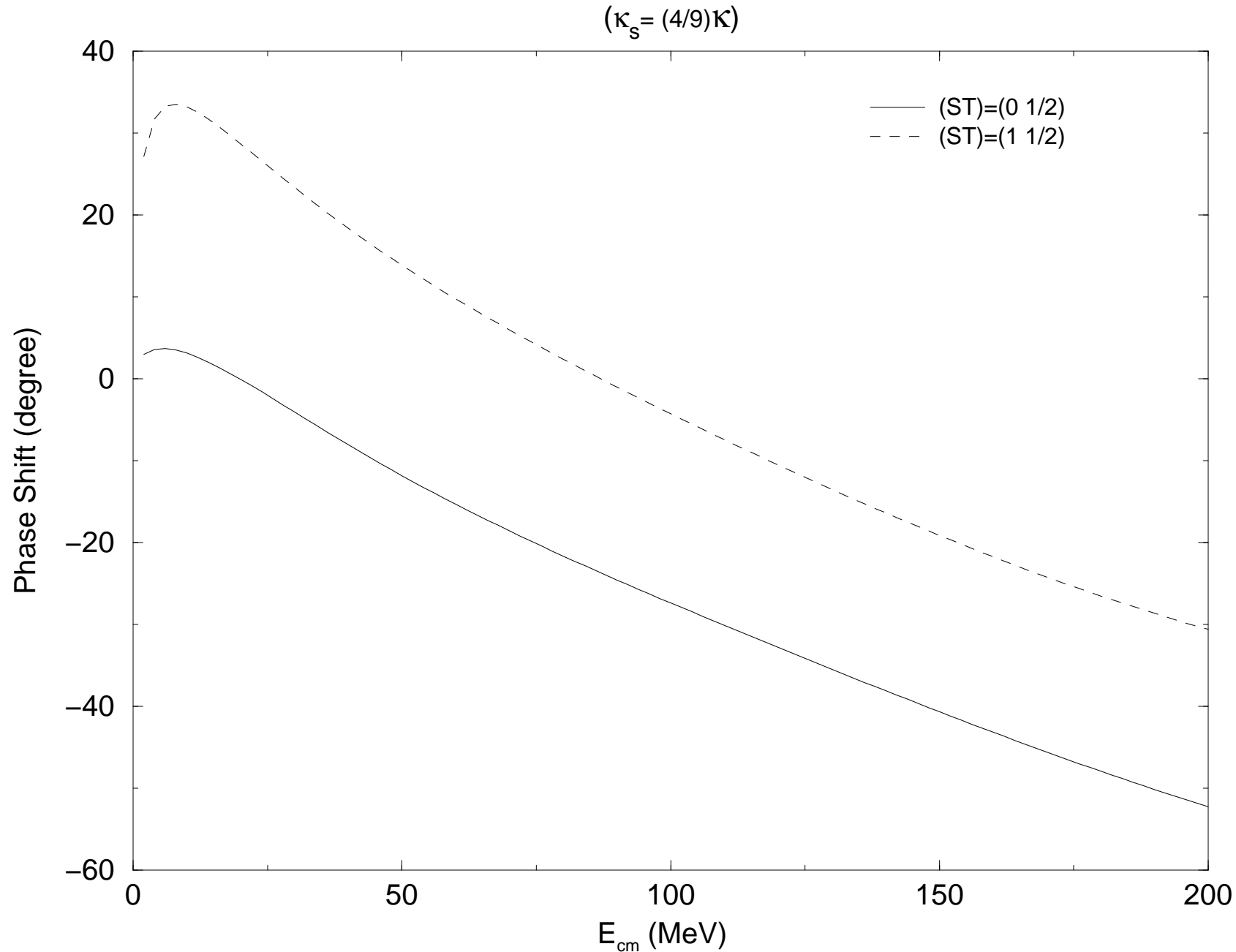


Fig.7  $N\Sigma$  Scattering Phase Shifts

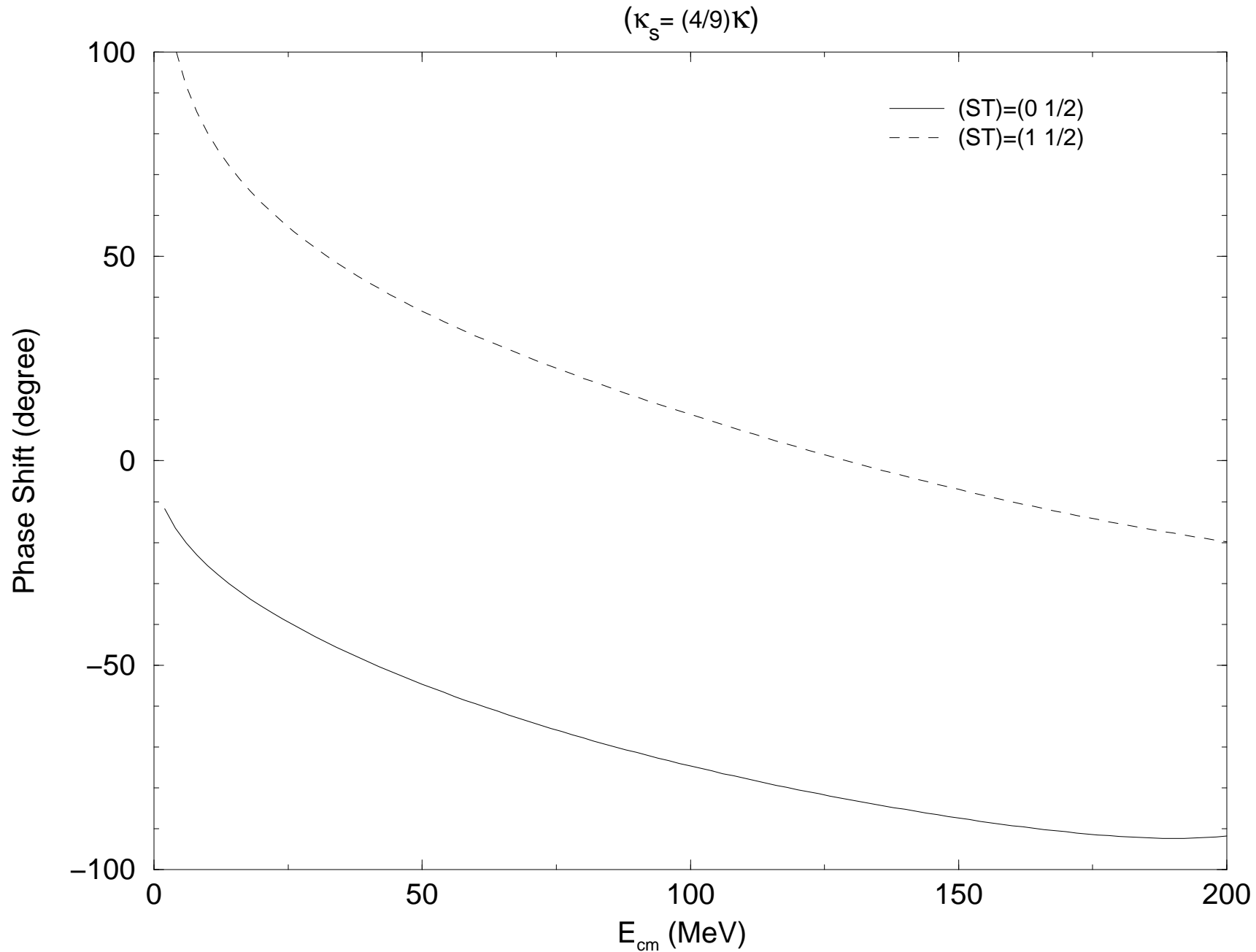
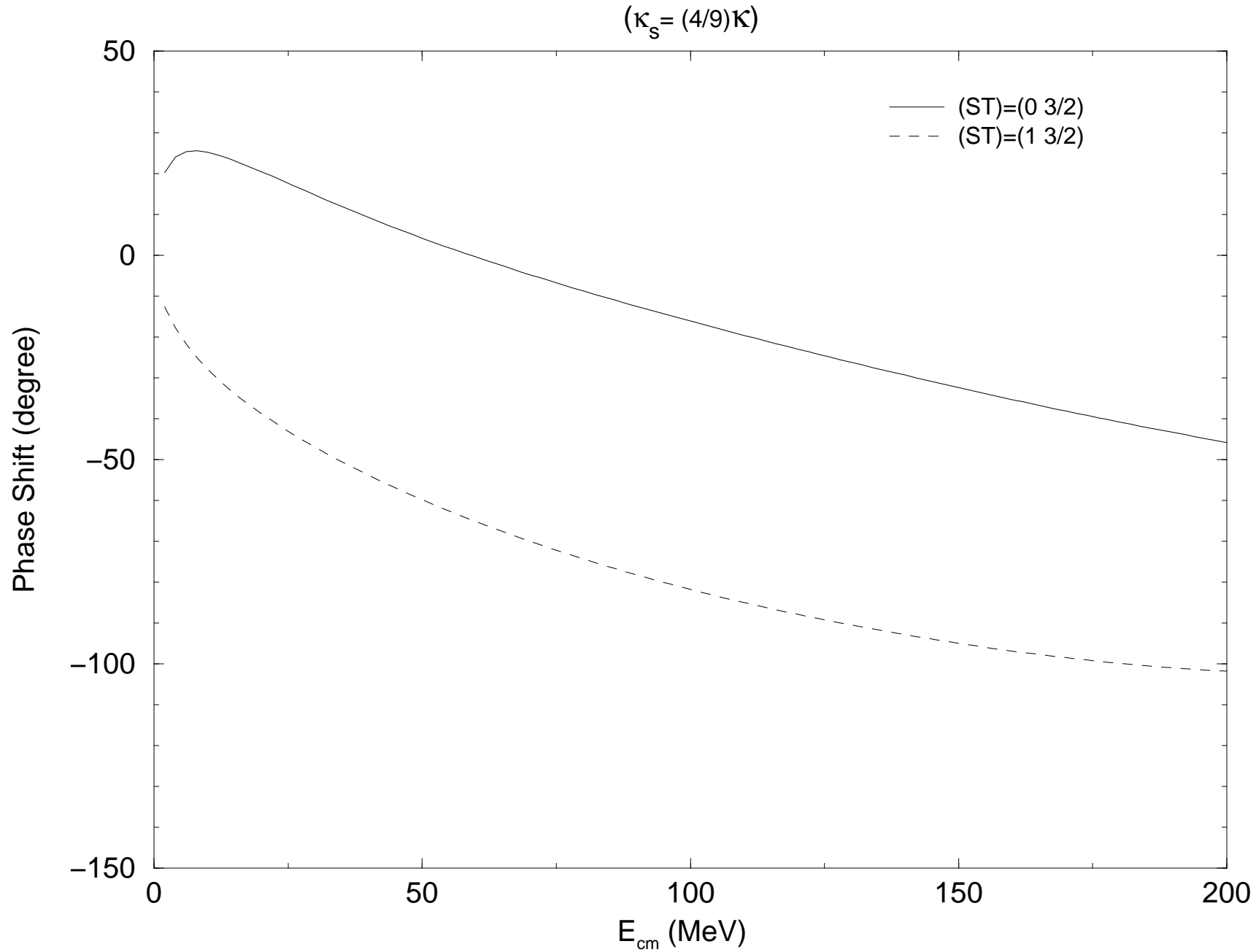


Fig.8  $N\Sigma$  Scattering Phase Shifts



# Fig.9 NΛ Scattering Cross–sections

